SOILS AND FOUNDATIONS Vol. 29, No. 3, 25-40, Sept. 1989
Japanese Society of Soil Mechanics and Foundation Engineering

A STUDY ON LATERAL DASHPOTS FOR SOIL-STRUCTURE INTERACTION AND ITS APPLICATION TO A SIMPLIFIED TECHNIQUE

NOBUO FUKUWA[i] and SHOICHI NAKAI[ii]

ABSTRACT

The dynamic characteristics of embedded rigid foundations are studied using the boundary element method. Lateral dashpots are introduced to the soil in plane strain in order to represent the wave propagation toward the third direction from a slice of the soil and their effects are examined. The impedance functions and foundation input motions are presented for the case of a rigid foundation embedded in a half-space or a stratum and for the case of two rigid foundations also embedded in a half-space. The effect of the lateral dashpots on the soil-structure interaction is studied where the embedment, the bedrock and the adjacent foundation are considered. The numerical examples are provided by comparing the results obtained by two-dimensional, approximate three-dimensional and exact three-dimensional analyses. The efficiency of the dashpots is confirmed, in particular, for a foundation embedded in a half-space. Based on this result, the lateral dashpots are introduced to one-dimensional soil columns which represent a half-space around an embedded foundation. From this assumption, the impedance functions are easily obtained in an explicit form and the foundation input motions are evaluated using the substructure technique. The validity of this simplified technique is confirmed by comparing its results with those obtained by a three-dimensional boundary element analysis.

Key words : damping, dynamic, earthquake, foundation, vibration, viscoelasticity, wave propagation (**IGC** : E 8/E 12)

INTRODUCTION

Dynamic soil-structure interaction analyses are often carried out with the aid of two-dimensional (2-D) representation due to large efforts involved in a realistic three-dimensional (3-D) modeling. However, Luco et al. (1974), Jakub (1977) and Kausel et al. (1974) have shown the difficulty of obtaining a good approximate solution by a 2-D analysis compared with the exact 3-D one. It has been pointed out that the imaginary part of impedance function in the 2-D modeling agrees well with that in the 3-D modeling

[i] Research Engineer, Ohsaki Research Institute, Shimizu Corporation, 2-2-2, Uchisaiwai-cho, Chiyoda-ku, Tokyo 100.
[ii] Senior Research Engineer, ditto.
Manuscript was received for review on June 8, 1988.
Written discussions on this paper should be submitted before April 1, 1990, to the Japanese Society of Soil Mechanics and Foundation Engineering, Sugayama Bldg. 4 F, Kanda Awaji-cho 2-23, Chiyoda-ku, Tokyo 101, Japan. Upon request the closing date may be extended one month.

however the real part is underestimated in the 2-D approximation. Consequently, damping is overestimated in the 2-D modeling and it gives an unconservative results. From this point of view, a method of approximate three-dimensional (approx. 3-D) analysis was proposed by Hwang et al. (1975) and applied to program FLUSH by Lysmer et al. (1975). In this analysis method, the 3-D effect is introduced by adding the lateral dashpots in order to account for shear wave propagation toward the third direction. In spite of the wide usage of these dashpots in dynamic response analyses, their effects on the soil-structure interaction have not been discussed in detail.

On the soil structure interaction, numerous works have been done since Lamb's work (1904). The state-of-the-art in this field was well documented by Gazetas (1983). The introduction of the previous works on the soil structure interaction, therefore, are not presented here.

In this paper, the effect of viscous forces introduced by Hwang et al. (1975) on the soil-structure interaction is examined through the impedance functions and foundation input motions of rigid foundations which are embedded in a homogeneous elastic half-space and a stratum overlying a rigid rock. First the Green's function for this problem is derived, then this Green's function is applied to the boundary element formulation in conjunction with the substructure technique. The effect of the dashpots on the soil-strucure interaction problem including the embedment, underlying bedrock and adjacent foundation are examined by comparing the results obtained by 2-D, approx. 3-D and exact 3-D analyses. In order to confirm the characteristics of wave propagation, the energy transmission from a line source is compared among the above mentioned three different methods. From this result, the efficiency of the dashpots for a problem of a rigid foundation in a half-space is recognized. These features of the approximate three-dimensional analysis have been demonstrated in the previous papers (Nakai and Fukuwa, 1984, 1987).

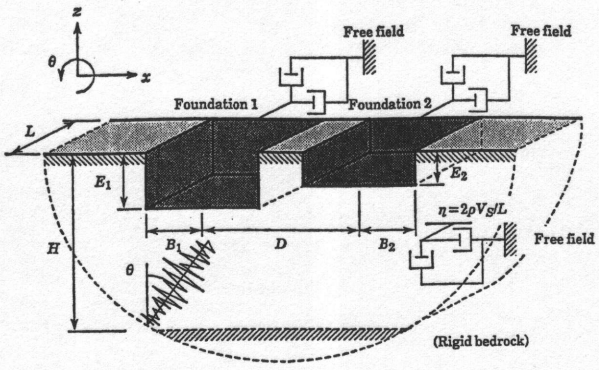

Fig. 1. Model for approximate three-dimensional boundary element analysis

A simplified technique evaluating the impedance functions and foundation input motions is proposed by applying the dashpots to soil columns which represent half-spaces around a foundation. The proposed method does not require any empirical insights which are often needed in existing simplified procedures. The present method can be applied to evaluate the foundation input motions as well as the impedance functions of embedded foundations. The simplified impedance formulation was first proposed by Lysmer (1965) in which the vertical impedance function can be represented by a single-degree-of-freedom mass-spring-dashpot model. Richart et al. (1970) also demonstrated a similar approximation for all four vibration modes. Meek and Veletsos (1974) improved this concept by introducing a fictious mass connected to a foundation through a dashpot. Wolf and Somaini (1986) extended Meek and Veletsos's work to the embedded foundations. These simplified techniques are limited to evaluating the impedance functions and are derived from the semi-empirical procedure in which simplified solutions are fitted to the exact one.

APPROXIMATE THREE-DIMENSIONAL BOUNDARY ELEMENT ANALYSIS FOR EMBEDDED RIGID FOUNDATIONS

Model and Method of Analysis

In order to study the effect of lateral dashpots

on the soil-structure interaction, the dynamic characteristics of embedded foundations subjected to SV waves are investigated using the boundary element method combined with the substructure technique. A soil-foundation model illustrated in Fig. 1 is considered in this section. The rigid foundation whose area is $2B\times L$ is embedded with depth E in a slice of soil with thickness L. The lateral dashpots are added to the soil slice in order to represent a 3-D effect in wave propagation. A stratum with depth H as well as a half-space are selected to examine the influence of the underlying bedrock. Besides the single foundation case, a case of two foundations with distance D is considered to study the effect of the structure-soil-structure interaction.

The viscous damping coefficient is introduced to the equation of motion for the scattering wave field in order to represent the dashpots. Using the time dependence of $e^{i\omega t}$, the displacement vector $\boldsymbol{u}^S$ satisfies the following equation :

$$(\lambda+\mu)\nabla\nabla\cdot\boldsymbol{u}^S+\mu\nabla^2\boldsymbol{u}^S+\rho\omega^2\boldsymbol{u}^S-i\omega\eta\boldsymbol{u}^S=0, \tag{1}$$

where ρ is the mass density of the ground, λ and μ are the complex Lamé's constants considering the hysteretic damping h_D, ∇ is the vector differential operator, and the superscript S stands for the scattering wave field. The viscous damping coefficient η, which is related to dashpots, is defined by

$$\eta=\frac{2\rho V_S}{L},\quad V_S=\left(\frac{|\mu|}{\rho}\right)^{1/2}, \tag{2}$$

where V_S is the absolute value of the complex shear wave velocity and the factor 2 in the first equation arises from the two faces of the model.

On the other hand, the equation of motion for the incident and reflected wave field is written as follows :

$$(\lambda+\mu)\nabla\nabla\cdot\boldsymbol{u}^I+\mu\nabla^2\boldsymbol{u}^I+\rho\omega^2\boldsymbol{u}^I=0, \tag{3}$$

where the superscript I denotes the incident and reflected wave field. In this equation, it must be pointed out that the damping term does not exist because the dashpots are effective only for the radiation toward the third direction from the slice of soil.

For the boundary element analysis, appropriate fundamental solutions are necessary. In order to avoid the additional boundary element discretization except for the soil-foundation interface, the Green's functions are derived here for a homogeneou shalf-space and a stratum overlying a rigid rock. The fundamental solution $\boldsymbol{u}_F=(u_F, w_F)$, which corresponds to the Green's function for an infinite domain, can be obtained by solving an equation :

$$(\lambda+\mu)\nabla\nabla\cdot\boldsymbol{u}_F+\mu\nabla^2\boldsymbol{u}_F+\rho\omega^2\boldsymbol{u}_F-i\omega\eta\boldsymbol{u}_F+\boldsymbol{f}\delta_i=\boldsymbol{0}, \tag{4}$$

where δ_i is the Dirac delta function, $\boldsymbol{f}=(p, q)$ is the point source vector, and the subsctipt F denotes the Green's function for a full-space. Eq. (4) can be solved by taking Fourier transforms with respect to x- and z-coordinates. The resultant displacement is written as follows (Love, 1927) :

$$\left.\begin{aligned}
u_F(x,z)=&\frac{i}{4\mu k^2}\left[\left\{\frac{\partial^2}{\partial x^2}H_0^{(2)}(hr)+\frac{\partial^2}{\partial z^2}H_0^{(2)}(kr)\right\}p+\frac{\partial^2}{\partial x\partial z}\right.\\
&\left.\times\{H_0^{(2)}(hr)-H_0^{(2)}(kr)\}\right],\\
w_F(x,z)=&\frac{i}{4\mu k^2}\left[\{H_0^{(2)}(hr)-H_0^{(2)}(kr)\}p+\frac{\partial^2}{\partial x\partial z}\left\{\frac{\partial^2}{\partial z^2}H_0^{(2)}(hr)\right.\right.\\
&\left.\left.+\frac{\partial^2}{\partial x^2}H_0^{(2)}(kr)\right\}\right],
\end{aligned}\right\} \tag{5}$$

in which $H_0^{(2)}$ is the Hankel function of the second kind of order zero and

$$\left.\begin{aligned}
&h^2=(\omega/c_P)^2-i\omega/d_P,\quad k^2=(\omega/c_S)^2-i\omega/d_S,\\
&c_P^2=(\lambda+2\mu)/\rho,\quad c_S^2=\mu/\rho,\\
&d_P=(\lambda+2\mu)/\eta,\quad d_S=\mu/\eta,\quad r^2=x^2+z^2,\\
&\alpha^2=\xi^2-h^2,\quad \beta^2=\xi^2-k^2.
\end{aligned}\right\} \tag{6}$$

Considering the boundary condition at a free surface and a rigid rock, the Green's function is obtained by applying the Fourier transform with respect to x-direction using the fundamental solution above mentioned. The Green's

function for a half-space is written as

$$\left.\begin{aligned} u=&\frac{1}{\pi\mu k^2}\int_0^\infty\Big[-p\frac{\xi^2\cos\xi x}{\alpha F_H(\xi)}((2\xi^2-k^2)e^{-\alpha z}\\ &-2\alpha\beta e^{-\beta z})\sigma'_z+q\frac{\xi\sin\xi x}{\pi F_H(\xi)}(-2\xi^2e^{-\alpha z}\\ &+(2\xi^2-k^2)e^{-\beta z})\tau'_z\Big]d\xi+u_F(x+f,z)\\ &+u_F(x-f,z),\\ w=&\frac{1}{\pi\mu k^2}\int_0^\infty\Big[p\frac{\xi\sin\xi x}{F_H(\xi)}((2\xi^2-k^2)e^{-\alpha z}\\ &-2\xi^2e^{-\beta z})\sigma'_z+q\frac{\xi^2\cos\xi x}{\beta F_H(\xi)}(-2\alpha\beta e^{-\alpha z}\\ &+(2\xi^2-k^2)e^{-\beta z})\tau'_z\Big]d\xi+w_F(x+f,z)\\ &+w_F(x-f,z),\end{aligned}\right\}\quad(7)$$

where f is the depth of a source and

$$\left.\begin{aligned}\sigma'&=(2\xi^2-k^2)e^{-\alpha f}-2\alpha\beta e^{-\beta f},\\ \tau'&=2\alpha\beta e^{-\alpha f}-(2\xi^2-k^2)e^{-\beta f},\end{aligned}\right\}\quad(8)$$

and the Rayleigh function $F_H(\xi)$ for the half-space is

$$F_H(\xi)=(2\xi^2-k^2)^2-4\alpha\beta\xi^2.\quad(9)$$

Considering a rigid rock, the Green's function is obtained as follows :

$$\left.\begin{aligned} u=&-\frac{1}{2\pi\mu}\int_0^\infty\frac{1}{F_R(\xi)}[p\cos\xi x\{i\xi(A_H'+C_H')\\ &+\beta(B_H'-D_H')\}+iq\sin\xi x\{i\xi(A_V'+C_V')\\ &+\beta(B_V'-D_V')\}]d\xi+u_F(x+f,z)\\ &+u_F(x-f,z),\\ w=&\frac{1}{2\pi\mu}\Big[\int_0^\infty\frac{1}{F_R(\xi)}[ip\sin\xi x\{\alpha(A_H'-C_H')\\ &-i\xi(B_H'+D_H')\}+q\cos\xi x\{\alpha(A_V'-C_V')\\ &-i\xi(B_V'+D_V')\}]d\xi+w_F(x+f,z)\\ &+w_F(x-f,z),\end{aligned}\right\}\quad(10)$$

in which integration constants $A_H\sim D_H$ and $A_V\sim D_V$ are obtained by solving

$$\frac{1}{2F_R(\xi)}\begin{bmatrix}2\xi^2-k^2 & -2i\beta\xi & 2\xi^2-k^2 & 2i\beta\xi\\ -2i\alpha\xi & -2\xi^2+k^2 & 2i\alpha\xi & -2\xi^2+k^2\\ i\xi e^{-\alpha H} & \beta e^{-\beta H} & i\xi e^{\alpha H} & \beta e^{-\beta H}\\ -\alpha e^{-\alpha H} & i\xi e^{-\beta H} & \alpha e^{\alpha H} & i\xi e^{-\beta H}\end{bmatrix}$$

$$\times\left(\begin{Bmatrix}A_H'e^{\alpha z}\\ B_H'e^{-\alpha z}\\ C_H'e^{\beta z}\\ D_H'e^{-\beta z}\end{Bmatrix},\begin{Bmatrix}A_V'e^{\alpha z}\\ B_V'e^{-\alpha z}\\ C_V'e^{\beta z}\\ D_V'e^{-\beta z}\end{Bmatrix}\right)=\left(\begin{Bmatrix}\sigma_H'\\ 0\\ u_H'\\ w_H'\end{Bmatrix},\begin{Bmatrix}0\\ \tau_V'\\ u_V'\\ w_V'\end{Bmatrix}\right),$$

where

$$\left.\begin{aligned} u_H'&=\frac{1}{2k^2}\Big\{\beta(e^{-(H-f)\beta}+e^{-(H-f)\beta})\\ &\quad-\frac{\xi^2}{\alpha}(e^{-(H+f)\alpha}+e^{-(H+f)\alpha})\Big\},\\ w_H'&=-\frac{i\xi}{2k^2}\{e^{-(H-f)\alpha}-e^{-(H-f)\beta}\\ &\quad+e^{-(H+f)\alpha}-e^{-(H+f)\beta}\},\\ \sigma_H'&=-\frac{i\xi}{k^2\alpha}\{(2\xi^2-k^2)e^{-\alpha f}-2\alpha\beta e^{-\beta f}\},\\ u_V'&=\frac{i\xi}{2k^2}\{e^{-(H-f)\alpha}-e^{-(H-f)\beta}\\ &\quad+e^{-(H+f)\alpha}-e^{-(H+f)\beta}\},\\ w_V'&=-\frac{1}{2k^2}\Big\{\alpha(e^{-(H-f)\alpha}+e^{-(H-f)\alpha})\\ &\quad-\frac{\xi^2}{\beta}(e^{-(H+f)\beta}+e^{-(H+f)\beta})\Big\},\\ \tau_V'&=-\frac{i\xi}{k^2\beta}\{2\alpha\beta e^{-\alpha f}-(2\xi^2-k^2)e^{-\beta f}\},\end{aligned}\right\}\quad(11)$$

and the Rayleigh function for this problem is

$$\begin{aligned}F_R(\xi)=&8\alpha\beta\xi^2(2\xi^2-k^2)+(\xi^2-\alpha\beta)\\ &\times\{(2\xi^2-k^2)^2-4\alpha\beta\xi^2\}\cosh(\alpha+\beta)H\\ &-(\xi^2+\alpha\beta)\{2\xi^2-k^2)^2+4\alpha\beta\xi^2\}\\ &\times\cosh(\alpha-\beta)H.\end{aligned}\quad(12)$$

The expression for the traction which is not presented here is easily obtained from displacements using the constitutive relation. The difference whether dashpots are considered or not exists only in the complex wave numbers h and k.

Considering a train of plane SV waves propagating in the x-z plane, the solutions for the incident wave field are easily obtained. In this procedure, the conventional method by Ewing et al. (1957) is employed in terms of potentials that satisfy Eq. (3).

The boundary element equation for the scattering wave field is obtained by applying the method of weighted residuals. The displacement vector $\boldsymbol{u}_i$ of point i at boundary Γ can be expressed in terms of boundary

values (Brebbia, 1980) :

$$\boldsymbol{C}_i \cdot \boldsymbol{u}_i^S + \int_\Gamma \boldsymbol{p}_{(k)}^* \cdot \boldsymbol{u}^S d\Gamma = \int_\Gamma \boldsymbol{u}_{(k)}^* \cdot \boldsymbol{p}^S d\Gamma, \tag{13}$$

in which $\boldsymbol{C}_i$ is the coefficient matrix depending on the geometry of boundary, $\boldsymbol{u}^*$ and $\boldsymbol{p}^*$ are the displacement and traction vectors corresponding to the weighting field. $\boldsymbol{u}^*$ and $\boldsymbol{p}^*$ correspond to the fundamental solutions satisfying the equation of motion Eq. (4) and those are already obtained as Eqs. (5), (7) and (10). $\boldsymbol{u}^S$ and $\boldsymbol{p}^S$ are the boundary values of the displacement and traction, respectively, and the subscript(k) denotes the dimension of space under consideration. As mentioned above, the usage of the Green's function which satisfies the boundary condition enables us to perform the integration in Eq. (13) only along the soil-foundation interface.

The total displacement and traction consist of the values in the scattering wave field and those in the incident and reflected wave field :

$$\boldsymbol{u} = \boldsymbol{u}^S + \boldsymbol{u}^I, \quad \boldsymbol{p} = \boldsymbol{p}^S + \boldsymbol{p}^I. \tag{14}$$

Eq. (13) is discretized on the assumption of constant variation of displacements and tractions over each boundary element as follows :

$$\boldsymbol{H}_{(k)} \cdot \boldsymbol{u} = \boldsymbol{G}_{(k)} \cdot \boldsymbol{p} + \boldsymbol{H}_{(k)} \cdot \boldsymbol{u}^I - \boldsymbol{G}_{(k)} \cdot \boldsymbol{p}^I, \tag{15}$$

in which

$$\left.\begin{aligned} \boldsymbol{H}_{ij(k)} &= \delta_{ij}\boldsymbol{C}_i + \int_{\Gamma_j} \boldsymbol{p}_{(k)}^* d\Gamma, \\ \boldsymbol{G}_{ij(k)} &= \int_{\Gamma_j} \boldsymbol{u}_{(k)}^* d\Gamma, \end{aligned}\right\} \tag{16}$$

where the coefficient matrix $\boldsymbol{C}_i$ is evaluated from the sum of all the off-diagonal coefficients of $\boldsymbol{H}$ matrix for the static problem, since the singularity is the same in the static and dynamic cases.

Consider the rigid massless foundations embedded in the soil as shown in Fig. 1. The compatibility of displacements on the contact area of a rigid foundation can be expressed by

$$\boldsymbol{u} = \boldsymbol{T} \cdot \boldsymbol{u}^F, \tag{17}$$

where $\boldsymbol{u}^F$ is the displacement vector at the centroid of the bottom of foundation. $\boldsymbol{T}$ is the transformation matrix which represents the relationship between the reduced displacements and the nodal displacements along the boundary. Introducing the diagonal matrix $\boldsymbol{A}$ which includes the area of each element, Eq. (15) can be rewritten by multiplying $\boldsymbol{T}^t \cdot \boldsymbol{A} \cdot \boldsymbol{G}^{-1}$ to the both sides of the equation :

$$\boldsymbol{K} \cdot \boldsymbol{u}^F = \boldsymbol{f}^E + \boldsymbol{f}^D, \tag{18}$$

where

$$\left.\begin{aligned} \boldsymbol{K} &= \boldsymbol{T}^t \cdot \boldsymbol{A} \cdot \boldsymbol{G}_{(k)}^{-1} \cdot \boldsymbol{H}_{(k)} \cdot \boldsymbol{T}, \\ \boldsymbol{f}^E &= \boldsymbol{T}^t \cdot \boldsymbol{A} \cdot \boldsymbol{p}, \\ \boldsymbol{f}^D &= \boldsymbol{T}^t \cdot \boldsymbol{A} \cdot (\boldsymbol{G}_{(k)}^{-1} \cdot \boldsymbol{H}_{(k)} \cdot \boldsymbol{u}^I - \boldsymbol{p}^I), \end{aligned}\right\} \tag{19}$$

in which $\boldsymbol{K}$ is the impedance matrix of fundations, $\boldsymbol{f}^E$ is the external force vector and $\boldsymbol{f}^D$ is the driving force vector. The foundation input motion vector, which corresponds to the response of a rigid massless foundation subjected to a seismic wave, is derived by substituting $\boldsymbol{f}^E = \boldsymbol{0}$ into Eq. (18).

For the approx. 3-D analysis, dashpot terms which represent the radiation to the third direction directly from the side walls of the foundations must be added when calculating impedance matrices and driving force vectors based on Eq. (19).

It is worthy of note that the expression of driving force in Eq. (19) differs from that of the conventional boundary element formulation, because the damping terms are added only for the scattering wave field as shown in Eq. (1) in the case of approx. 3-D analysis. The discretized boundary integral equation in the incident and reflected wave field is written as

$$\boldsymbol{H}_{(2\text{-D or } 3\text{-D})} \cdot \boldsymbol{u}^I = \boldsymbol{G}_{(2\text{-D or } 3\text{-D})} \cdot \boldsymbol{p}^I + \boldsymbol{u}^I. \tag{20}$$

Substituting Eq. (20) into Eq. (19), the driving force vector is expressed by

$$\boldsymbol{f}^D = \boldsymbol{T}^t \cdot \boldsymbol{A} \cdot (\boldsymbol{G}_{(k)}^{-1} \cdot \boldsymbol{H}_{(k)} \cdot \boldsymbol{u}^I - \boldsymbol{G}_{(2\text{-D or } 3\text{-D})}^{-1} \times \boldsymbol{H}_{(2\text{-D or } 3\text{-D})} \cdot \boldsymbol{u}^I + \boldsymbol{G}_{(2\text{-D or } 3\text{-D})} \cdot \boldsymbol{u}^I). \tag{21}$$

Since the dimension of the scattered wave field (k) is identical with that of the incident and reflected wave field in case of 2-D or 3-D analysis, the first and second terms in the parenthesis of the right-hand side of

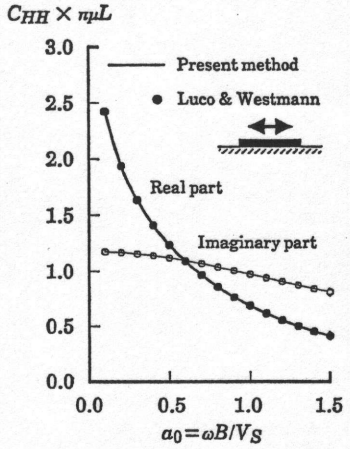

Fig. 2. Two-dimensional compliance function

Eq. (21) are cancelled out each other and then,

$$f^D = \boldsymbol{T}^t \cdot \boldsymbol{A} \cdot \boldsymbol{G} \cdot \boldsymbol{u}^I, \qquad (22)$$

which is the familiar expression for the driving force. When considering the viscous dashpots for approx. 3-D analysis, however, the driving force must be expressed by Eq. (19).

To verify the procedure presented above, the compliance function is compared with the result presented by Luco et al. (1972) in case of a surface foundation on a half-plane which has no viscous and hysteretic damping. Fig. 2 is a plot of the normalized compliance function for the horizontal translation for Poisson's ratio of 0.25. This figure clearly exhibits validity of the present method.

Numerical Results and Discussion

The effect of the dashpots on the soil-structure interaction problem including the embedment, underlying bedrock and adjacent foundation are examined by comparing the results obtained by 2-D, approx. 3-D and exact 3-D analyses. The 3-D solutions are derived from the results for rectangular foundations embedded in a half-space obtained by Yoshida and Kawase (1986) based on the boundary element method, and the results for a cylindrical foundation embedded in a stratum obtained by Fukuwa et al. (1984) based on the axisymmetric finite element method.

The square rigid foundation ($L=2B$) embedded with depth $E=B/2$ in a half-space, and Poisson's ratio of 0.4 is considered. Fig. 3 shows the dependency of normalized impedance function on the nondimensional frequency a_0 ($=\omega B/V_S$) while Fig. 4 provides the foundation input motion due to a vertically incident SV wave in the form of transfer function. It is found from these figures that the existence of viscous dashpots exerts a significant influence on the dynamic characteristics of a rigid foundation. The real part of the impedance function moves upward and approaches to that of exact 3-D solutions. The imaginary part also approaches to that of 3-D solutions except for the rocking impedance. This phenomenon in the imaginary part is mainly due to the dashpots added to the side walls of a foundation. Consequently, the equivalent damping ratio, which is half the ratio of the imaginary part to the real part, decreases and approaches to 3-D one. As an example, the equivalent damping ratio of the horizontal impedance is presented in Fig. 3 (e). There is a tendency that the real part is underestimated while the imaginary part is overestimated in the low frequency range particularly for the rotational mode. This implies that unconservative response is expected when the rotational response is dominant. For the foundation input motion, the viscous dashpots similarly enable 2-D solution to approach 3-D one. As a whole, it can be noted that the viscous dashpots produces their desired effects both on the impedance function and on the foundation input motion.

Next, the effect of dashpots on the underlying bedrock is investigated. The depth of rigid rock $H=4B$ is assumed, and the geometry of a foundation is selected to be identical with the previous one. The hysteretic damping ratio $h_D=0.05$ is used for a soil to avoid the singularity due to resonance. The horizontal impedance function and foundation input motion subjected to a SV wave are demonstrated in Figs. 5 and 6, respectively. These figures show that the viscous dashpots drastically suppress the fluctuation due to the existence of the be-

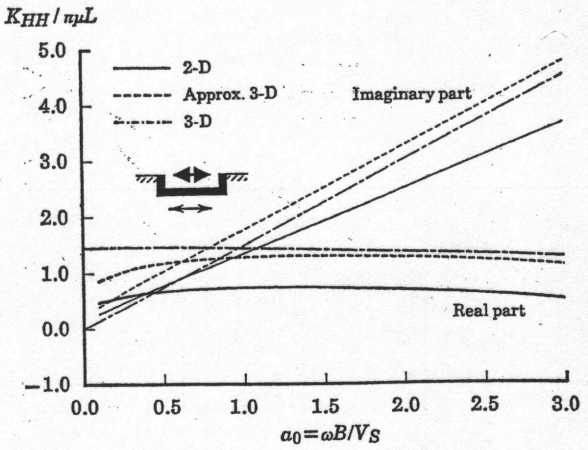

(a) Horizontal impedance function

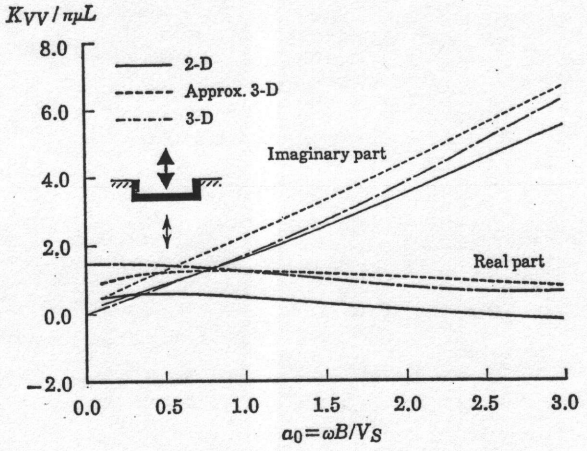

(c) Vertial impedance function

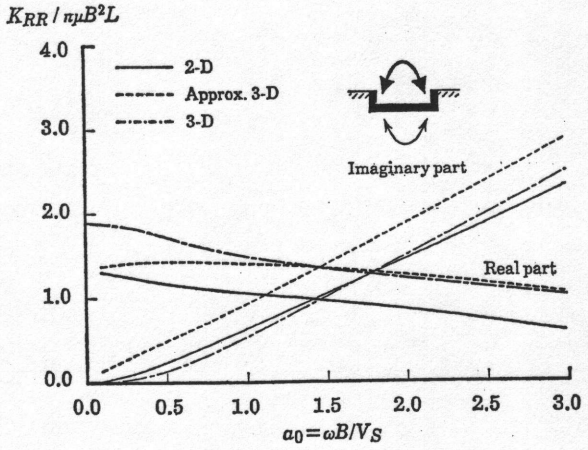

(b) Rotational impedance function

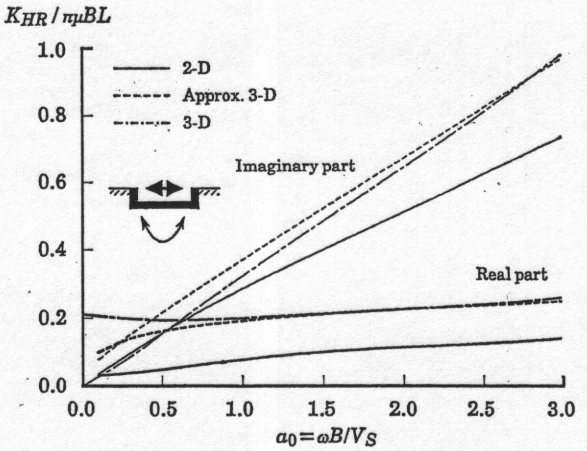

(d) Horizontal-rotational coupling impedance function

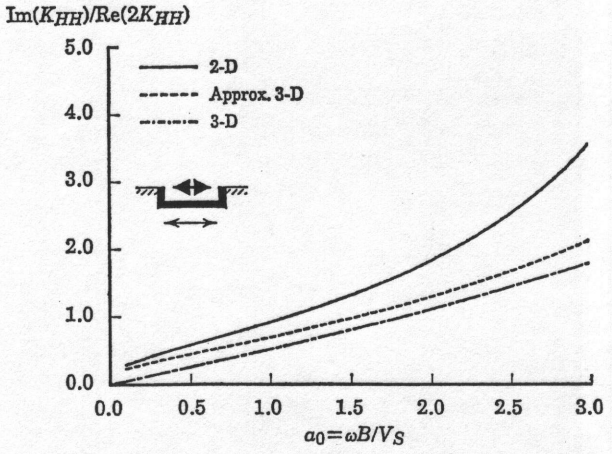

(e) Equivalent damping ratio of horizontal impedance function

Fig. 3. Impedance functions of an embedded foundation ($\nu=0.4$, $E/B=0.5$, half-space, $D/B=\infty$)

drock and the results almost coincide with those for a half-space. However the fluctuation is clearly recognized in the results for a circular foundation. This implies the disadvantage of the viscous dashpots ; i. e. the dashpots reduce the effect of bedrock and

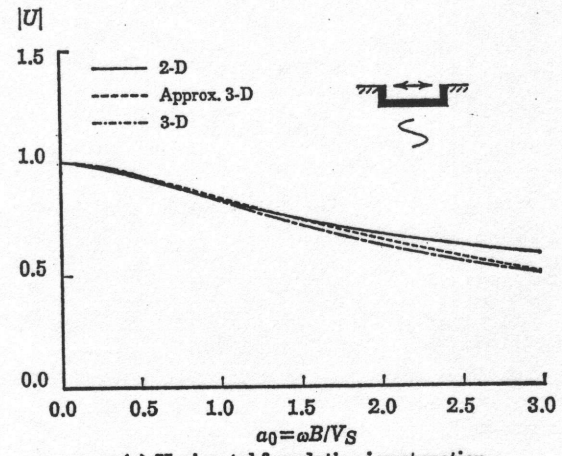

(a) Horizontal foundation input motion

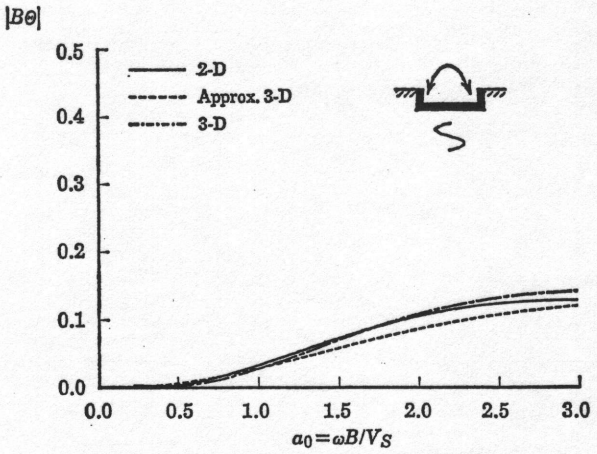

(b) Rotational foundation input motion

Fig. 4. Foundation input motions of an embedded foundation ($\nu=0.4$, $E/B=0.5$, $H/B=\infty$, $D/B=\infty$)

overestimate the radiation damping in the frequency below the cut-off frequency ($a_0=\pi/8$). However in a finite element analysis, it may turn out to be advantageous since a bad influence of an artificial bottom boundary inevitably assumed may be reduced. The underestimation of a bedrock influence is considered due to the excessive wave radiation toward the third direction, and this fact will be studied later by examining characteristics of wave propagation measured by the energy transmission.

Consider the two identical foundations at a distance of $D=3B/2$. The geometry of foundations is the same as the previous case and the soil is assumed to be a half-space. The horizontal and rotational impedances are

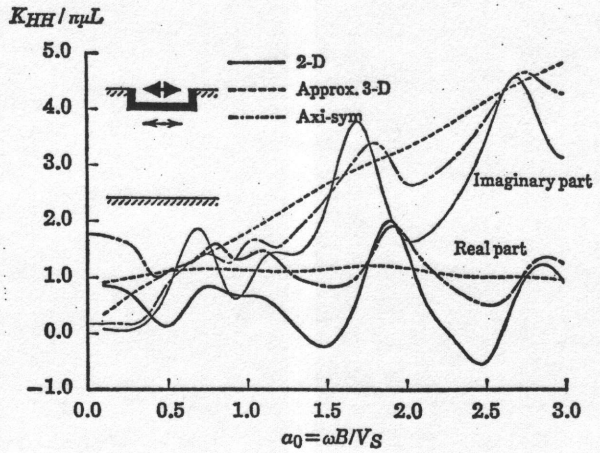

Fig. 5. Horizontal impedance function considering underlying bedrock ($\nu=0.4$, $E/B=0.5$, $H/B=4.0$, $D/B=\infty$, $h=0.05$)

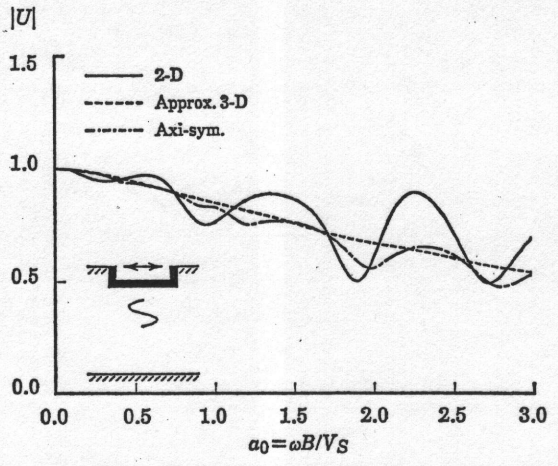

Fig. 6. Horizontal foundation input motion considering underlying bedrock ($\nu=0.4$, $E/B=0.5$, $H/B=4.0$, $D/B=\infty$, $h=0.05$)

demonstrated in Fig. 7 and the corresponding foundation input motions are shown in Fig. 8. The real part of impedance functions in Fig. 7 is larger than that for the single foundation in Fig. 3, while the imaginary part exhibits an opposite tendency due to wave reflection at a neighboring foundation. The influence of an adjacent foundation depends on the dimension of space. For 2-D case, the impedance function is affected by the adjacent foundation much stronger than that for other cases. This is due to the absence of radiation toward the third direction. The approx. 3-D results show that

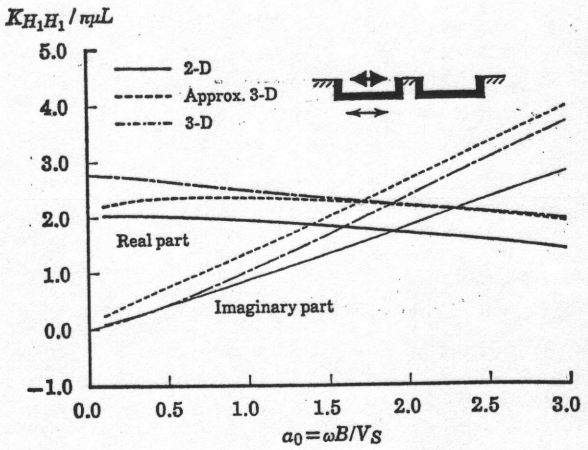

(a) Horizontal impedance function

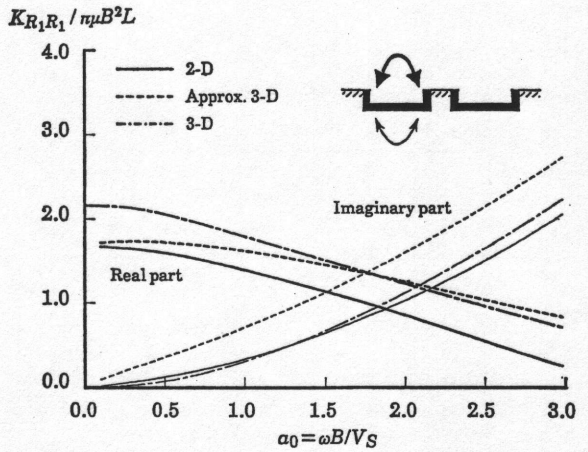

(b) Rotational impedance function

Fig. 7. Impedance functions considering an adjacent foundation ($\nu=0.4$, $E/B=0.5$, half-space, $D/B=2.5$)

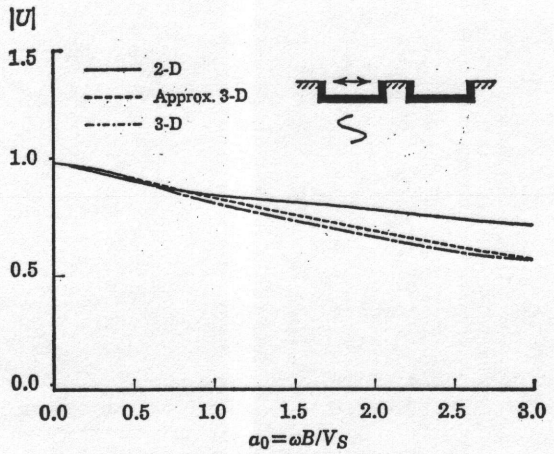

(a) Horizontal foundation input motion

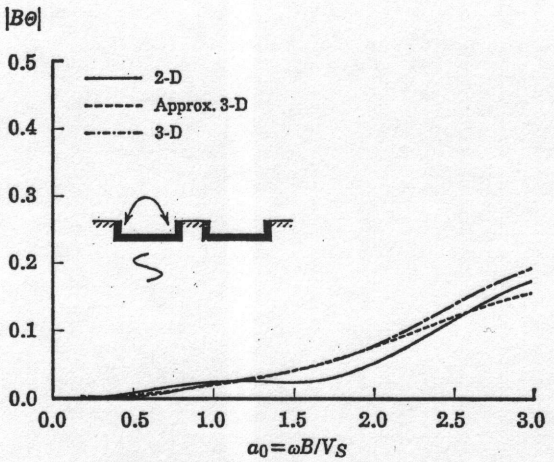

(b) Rotational foundation input motion

Fig. 8. Foundation input motions considering an adjacent foundation ($\nu=0.4$, $E/B=0.5$, half-space, $D/B=2.5$)

the effect of structure-soil-structure interaction is underestimated compared with the 3-D case. For the foundation input motion, it is also observed that the addition of dashpots makes its result close to the 3-D one while the fluctuation diminishes. This is recognized especially in the rotational mode which tends to be exerted by the existence of a neighboring foundation. This is due to the fact that the additional dashpots excessively absorb radiating waves from the foundation.

In order to examine the excessive wave radiation toward the third direction when viscous dashpots are added, the characteristics of wave propagation from a line source are discussed by evaluating the rate of energy transmission. The average flow of energy over one period through the surface S is defined by (Pao and Mow, 1973)

$$E=\iint_S \frac{1}{4} i\omega n_i(\sigma_{ij}\bar{u}_j-\bar{\sigma}_{ij}u_j)\,dS \qquad (23)$$

in which $\boldsymbol{n}$ is a unit normal vector and the upper bar denotes the complex conjugate. In the above equation, the summation convention is used. The integrand in Eq. (23) is the actual rate of work done by the surface traction per unit area averaged over one period and equal to the flow of energy. Considering a line source of length L at the surface, the average of energy flow at the concentric semi-cylindrical surface of radius

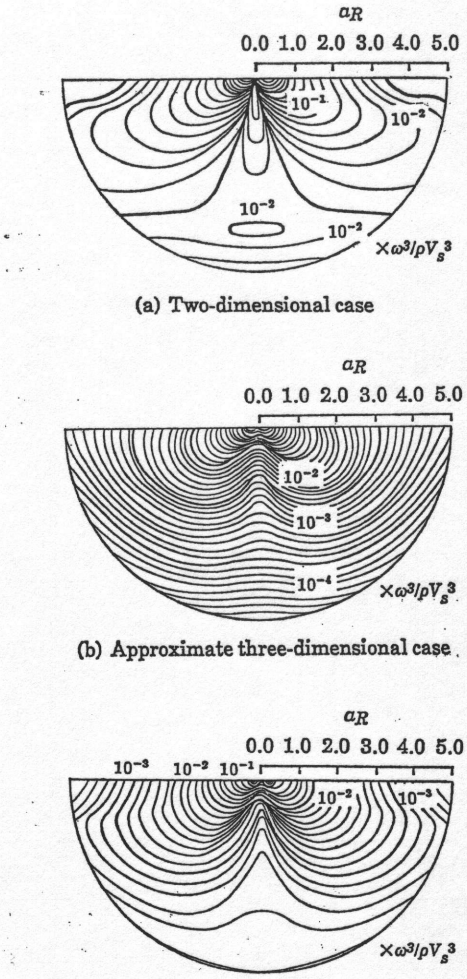

Fig. 9. Distribution of rate of energy transmission from horizontal line source (ν=0.4, half-space)

R and length L is expressed as follows :

$$E=\int_0^{\pi}\int_{-L/2}^{L/2}\frac{i\omega}{4}n_i(\sigma_{ij}\bar{u}_j-\bar{\sigma}_{ij}u_j)drRd\theta, \quad (24)$$

in which the displacement and stress are calculated using the Green's functions of a half-space for each dimension (Nakai et al., 1984 a ; Matsuoka and Yahata, 1980).

Fig. 9 shows the dependency of the integrand in Eq. (24) for a horizontal line source on the nondimensional distance $\alpha_R(=R\omega/V_S)$ when $\alpha_L(=L\omega/V_S)=1.0$. It is found in this figure that the distribution of the rate of energy transmission differs among the cases. The result for 2-D case exhibits less attenuation since the waves propagate only within a plane. The difference between the results

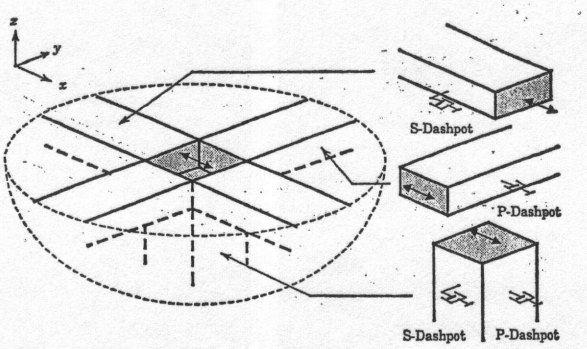

(a) Modeling of half-space by soil columns (b) Modeling of each soil column

Fig. 10. Representation of half-space by soil columns

for the approx. 3-D and exact 3-D cases is observed in the far region. This fact shows that the influence of distant objects such as a bedrock or adjacent structures becomes stronger for 2-D case while it diminishes for approx. 3-D case.

From the discussion described above, it can be concluded that the viscous dashpots fairly improve the 2-D results and make them approach to the 3-D ones especially for a foundation embedded in a homogeneous half-space. However it is also found that the effect of a bedrock and an adjacent foundation tends to be suppressed. Hence the approx. 3-D analysis must be used carefully when evaluating the effect of the layered soil or the structure-soil-structure interaction. Although the numerical results are presented only for the case of the Poisson's ratio ν= 0.4, we have confirmed that the conclusions demonstrated here do not change for the other Poisson's ratio.

SIMPLIFIED METHOD USING SOIL COLUMNS WITH DASHPOTS

As a result of the examination on the effect of the viscous dashpots for the soil-structure interaction, the efficiency of the dashpots is observed especially in the case of a foundation embedded in a half-space. Based on this fact, the method of simplified soil-structure interaction analysis is presented here by applying the dashpots to a one-dimensional (1-D) soil column.

Soil Column Model of Half-Space

The homogeneous half-space is partitioned into semi-infinite soil columns cennected to an embedded rigid foundation as shown in Fig. 10. In order to represent the 3-D wave radiation, the viscous dashpots are added to the surface around the soil column beneath the foundation and added to the both sides of the soil columns connected to side walls of the foundation. The representation of a soil by soil columns is similar to the model by Pauw (1953) which presented the static soil coefficients using the soil column with an expanding cross section. Gazetas et al. (1984) also used the soil column to represent the soil coefficients of piles.

Impedance Function of Surface Foundation

The impedance functions of the soil column with the dashpots are easily derived from the 1-D equation of motion. Considering the horizontal mode, the equation for the shear wave is written as

$$V_S^2\frac{\partial^2 u}{\partial z^2}=\frac{\eta}{\rho}\frac{\partial u}{\partial t}+\frac{\partial^2 u}{\partial t^2}, \tag{25}$$

in which η is the damping coefficient related to the dashpots. Considering the radiation condition, the impedance function is obtained by solving Eq. (25) as follows :

$$\left.\begin{aligned} &K_x=-\rho V_S^2 A\frac{\partial u}{\partial z}\Big|_{z=0}=\rho V_S^2 A\beta_x,\\ &\text{and}\quad \beta_x=\sqrt{-(\omega/V_S)^2+i\omega\eta/\rho V_S^2}, \end{aligned}\right\} \tag{26}$$

in which A $(=4BD)$ is the area of the foundation, B and D is a half width and a half depth of the foundation, and the sub-

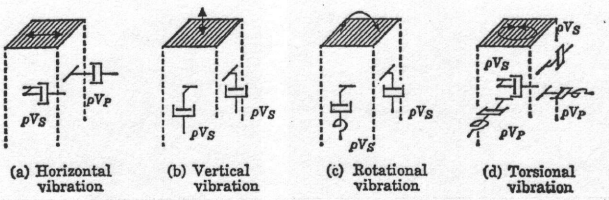

(a) Horizontal vibration (b) Vertical vibration (c) Rotational vibration (d) Torsional vibration

Fig. 11. Dashpots added to soil columns

Table 1. Impedance functions of soil column

Direction	Equation of motion	Impedance function	Spring const.	Damp. coef.	η(2−D)	η(3−D)
Horizontal(x)	$V_S^2\frac{\partial^2 u}{\partial z^2}=\frac{\eta}{\rho}\frac{\partial u}{\partial t}+\frac{\partial^2 u}{\partial t^2}$	$i\omega\rho V_S A\sqrt{1-\frac{i\eta}{\rho\omega}}$	$\frac{V_S}{2}\eta A$	$\rho V_S A$	$\frac{\rho V_L}{B}$	$\frac{\rho V_L}{B}+\frac{\rho V_S}{D}$
Vertical(z)	$V_L^2\frac{\partial^2 w}{\partial z^2}=\frac{\eta}{\rho}\frac{\partial w}{\partial t}+\frac{\partial^2 w}{\partial t^2}$	$i\omega\rho V_L A\sqrt{1-\frac{i\eta}{\rho\omega}}$	$\frac{V_L}{2}\eta A$	$\rho V_L A$	$\frac{\rho V_S}{B}$	$\frac{\rho V_S}{B}+\frac{\rho V_S}{D}$
Rotational(θ_y)	$V_L^2\frac{\partial^2\phi_y}{\partial z^2}-\frac{6}{5}\frac{A}{I_y}V_S^2\phi_y=\frac{\eta}{\rho}\frac{\partial\phi_y}{\partial t}+\frac{\partial^2\phi_y}{\partial t^2}$	$i\omega\rho V_L I_y\sqrt{1-\frac{18V_S^2}{5B^2\omega^2}-\frac{i\eta}{\rho\omega}}$	$1.9\frac{\rho V_S V_L}{B}I_y$	$\rho V_L I_y$	$\frac{3\rho V_S}{B}$	$\frac{3\rho V_S}{B}+\frac{\rho V_S}{D}$
Torsional(θ_z)	$V_S^2\frac{\partial^2\phi_z}{\partial z^2}=\frac{\eta}{\rho}\frac{\partial\phi_z}{\partial t}+\frac{\partial^2\phi_z}{\partial t^2}$	$i\omega\rho V_S I_z\sqrt{1-\frac{i\eta}{\rho\omega}}$	$\frac{V_S}{2}\eta I_z$	$\rho V_S I_z$	$\frac{3\rho V_S B^2+\rho V_L D^2}{(B^2+D^2)B}$	$\frac{3\rho V_S BD(B+D)+\rho V_L(B^3+D^3)}{(B^2+D^2)BD}$

$A=4BD$, $I_y=4B^3D/3$, $I_z=4BD(B^2+D^2)/3$

Table 2. Spring constants and damping coefficients of soil columns

Direction	Bottom Basement		x-dir. side wall		y-dir. side wall	
	K_B	C_B	K_X	C_X	K_Y	C_Y
x	$2\mu(B+\upsilon D)$	$\rho V_S A_B$	$\mu\upsilon E$	$\rho V_L A_X$	$\mu\upsilon E$	$\rho V_S A_Y$
y	$2\mu(D+\upsilon B)$	$\rho V_S A_B$	$\mu\upsilon E$	$\rho V_S A_X$	$\mu\upsilon E$	$\rho V_L A_Y$
z	$2\mu\upsilon(B+D)$	$\rho V_L A_B$	μE	$\rho V_S A_X$	μE	$\rho V_S A_Y$
θ_x	$2.53\mu\upsilon BD^2$	$\rho V_L I_{Bx}$	$\mu E(12D^2+\upsilon E^2)/12$	$\rho V_S I_{Xx}$	$0.63\mu\upsilon BE^2$	$\rho V_L I_{Yx}$
θ_y	$2.53\mu\upsilon B^2D$	$\rho V_L I_{By}$	$0.63\mu\upsilon DE^2$	$\rho V_L I_{Xy}$	$\mu E(12B^2+\upsilon E^2)/12$	$\rho V_S I_{Yz}$
θ_z	$2\mu\{3BD(B+D)+\upsilon(B^3+D^3)\}/3$	$\rho V_S I_{Bz}$	$1.26\mu\upsilon D^2E$	$\rho V_L I_{Xz}$	$1.26\mu\upsilon B^2E$	$\rho V_L I_{Yy}$
Others	$A_B=4BD$ $I_{Bx}=\frac{4BD^3}{3}$ $I_{By}=\frac{4DB^3}{3}$ $I_{Bz}=I_{Bx}+I_{By}$ $\upsilon=V_L/V_S$		$A_X=2DE$ $I_{Xx}=\frac{2ED^3}{3}$ $I_{Xy}=\frac{DE^3}{6}$ $I_{Xz}=I_{Xx}+I_{Xy}$		$A_Y=2BE$ $I_{Yx}=\frac{BE^3}{6}$ $I_{Yy}=\frac{2EB^3}{3}$ $I_{Yz}=I_{Yx}+I_{Yy}$	

Table 3. Spring constants and damping coefficients of embedded square foundation

Direction	Spring constants	Damping coefficients
Horizontal	$2\mu B\{(1+v)+2vE\}$	$4\rho V_S B\{B+(1+v)E\}$
Vertical	$4\mu\{vB+E\}$	$4\rho V_S B\{vB+2E\}$
Rotational	$\mu\left\{2.53vB^3+4B^2E+\frac{7}{6}vE^3+1.26vBE^2)\right\}$	$\frac{4\rho V_S B}{3}\{vB^3+(1+v)E^3+4B^2E\}$
Torsional	$\frac{4\mu}{3}\{(3+v)B^3+6.79vB^2E\}$	$\frac{8\rho V_S B^3}{3}\{B+(3+v)E\}$
Horizontal-Rotational	$2\mu vE^2$	$2\rho V_S(1+v)BE^2$

script x denotes the x-direction. The damping coefficient η for the 3-D case is defined by considering the dashpot for P-wave propagating toward the x-direction and that for S-wave propagating toward the y-direction as shown in Fig. 11 (a) :

$$\eta=\rho V_L/B+\rho V_S/D, \qquad (27)$$

where V_L is the analog wave velocity proposed by Lysmer (1965) and it has proven useful for understanding a surface foundation subjected to the vertical loading. The reason why the analog wave velocity is used instead of the usual P-wave velocity is to avoid the tendency that it becomes infinity when Poisson's ratio approaches to 0.5 as discussed by Gazetas et al. (1984). The Lysmer's analog wave velocity is written as

$$V_L=3.4\,V_S/\pi(1-\nu). \qquad (28)$$

The impedance functions for the other directional modes can be derived from the similar procedure. The equations of motion considered for these modes and the resultant impedance functions are listed in Table 1 in conjunction with the 2-D case.

Note that η for the 3-D case includes an additional term with that for the 2-D case. Therefore the spring constants, which are related to η, increase while the damping coefficients remain unchanged. From these results, it may be understood that only the real part of the impedance functions is affected by the viscous dashpots in the approx. 3-D analysis.

Impedance Function of Embedded Foundation

The contribution of the lateral soil must be taken into account when considering the embedment. This is easily evaluated by applying the impedance functions of the bottom soil column for the 2-D case in Table 1 ; i. e. replacing B and D with D and $E/2$ for the x-direction and with B and $E/2$ for the y-direction.

The impedance function of an embedded foundation can be obtained by summing up the contribution of the bottom and four lateral soil columns. From the view point of applying this method to the time domain analysis, the dynamic impedance functions are approximated by the spring constants and damping coefficients, which are independent of frequency, as presented in Table 1. These constants are calculated as asymptotic values when the frequency approaches infinity except for a rocking impedance which has a static value. The value of each soil column for each direction is exhibited in Table 2. Also, the resultant constants for a square embedded foundation, which are obtained by combining the values in Table 2 considering the foundation configuration, are listed in Table 3.

In order to examine the validity of the proposed method, a square foundation embedded with a height $E=B/2$ and B in a half-space of Poisson's ratio 0.4 is studied. The comparison between the result by the present method and that by the 3-D boundary element method is made in Fig. 12. It is seen from this figure that the present method provides a good approximation of an analytical one as a whole. However a slight difference is observed in a high frequency range especially for the case of $E=B$, since the impedance function based on the present

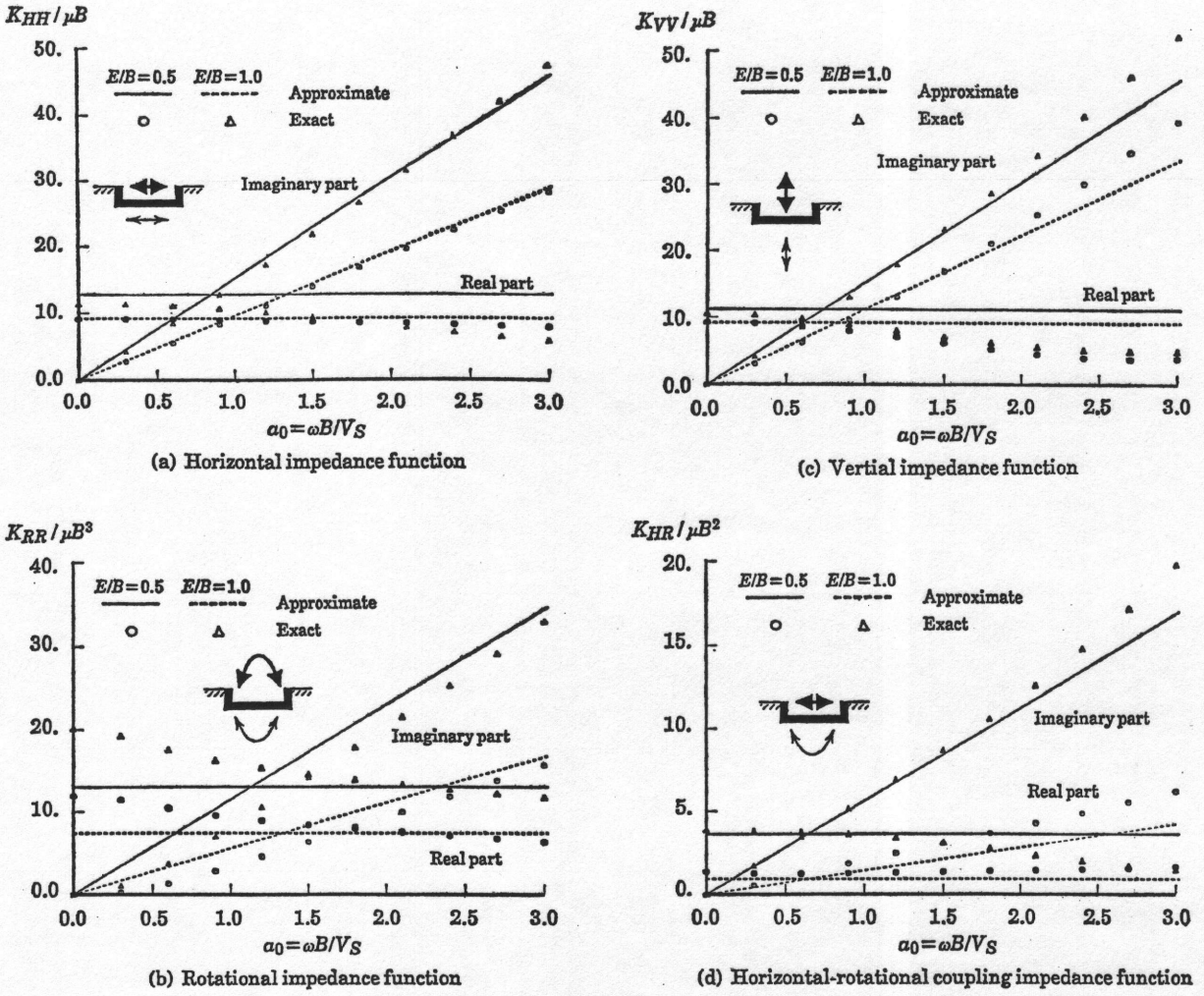

Fig. 12. Impedance functions by simplified technique ($\nu=0.4$)

method does not exhibit the frequency dependency. From this point of view, the application of this method to evaluate the impedance functions is efficient in the frequency range below the value $V_S/4B$ (corresponding to $a_0=\pi/2$). As a slight difference is recognized in the rotational impedance function, this method is normally applicable for the system in which translational modes are dominant.

Foundation Input Motion

Next, the foundation input motions due to SV waves are presented. Referring to Eqs. (18) and (19) considering the direction of normal vector, the foundation input motion $\boldsymbol{u}_G$ can be evaluated from the impedance matrix and the incident and reflected wave field :

$$\boldsymbol{u}_G=\boldsymbol{T}_G\cdot(\boldsymbol{u}^F+\boldsymbol{K}_G^{-1}\cdot\boldsymbol{p}^F)=\boldsymbol{T}_G \times\left(\begin{Bmatrix}\boldsymbol{u}_X^F\\ \boldsymbol{u}_Y^F\\ \boldsymbol{u}_B^F\end{Bmatrix}+\begin{bmatrix}\boldsymbol{K}_X & & \\ & \boldsymbol{K}_Y & \\ & & \boldsymbol{K}_B\end{bmatrix}^{-1}\cdot\begin{Bmatrix}\boldsymbol{p}_X^F\\ \boldsymbol{p}_Y^F\\ \boldsymbol{p}_B^F\end{Bmatrix}\right), \tag{29}$$

where $\boldsymbol{K}_G$ is the impedance matrix whose components are listed in Table 2, and $\boldsymbol{u}^F$ and $\boldsymbol{p}^F$ are the displacement and excavation force vectors of the free field. The excavation force vector corresponds to the force to excavate the soil and are evaluated by performing the integration of tractions along the soil-foundation interface. The transformation matrix $\boldsymbol{T}_G$ is introduced to consider the geometry of the rigid foundation. When a rigid foundation embedded in a half-space due to a vertically incident SV wave is selected, only a displacement to x-direction

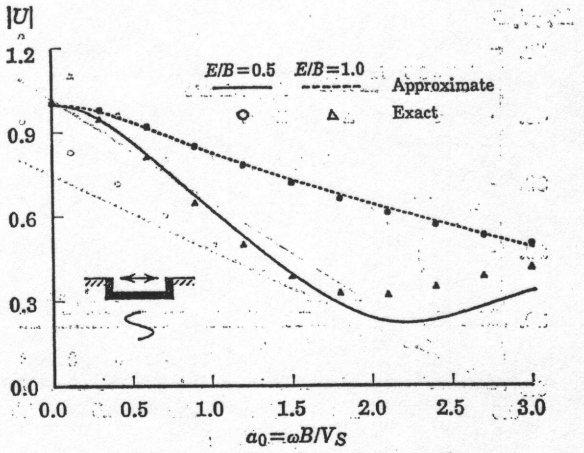

(a) Horizontal foundation input motion

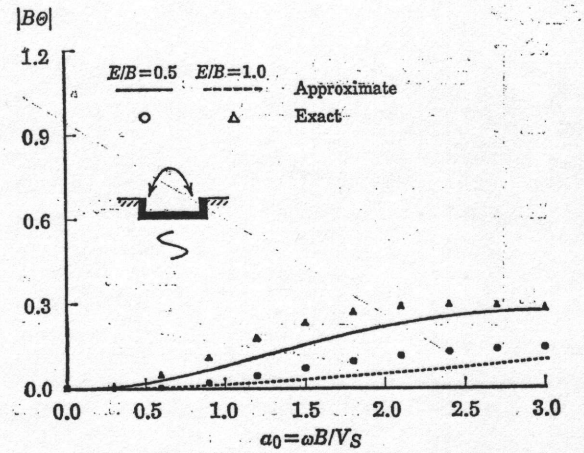

(b) Rotational foundation input motion

Fig. 13. Foundation input motions by simplified technique ($\nu=0.4$)

exists in the incident and reflected wave field :

$$u_x^F = U\cos(\omega z/c_S), \tag{30}$$

in which U is the displacement at the free surface. Denoting the averaged values of displacements along the bottom and side walls as $\boldsymbol{u}^F$ and the integrated values of tractions as $\boldsymbol{p}^F$, the non-zero values of the bottom are written as

$$\left.\begin{aligned} &u_{Bx}^F = U\cos(\xi E) \\ &\text{and } p_{Bx}^F = -4\mu U\xi BD\sin(\xi E), \end{aligned}\right\} \tag{31}$$

and those of side walls are

$$\left.\begin{aligned} &u_{Xx}^F = u_{Yx}^F = U\sin(\xi E)/\xi E \\ &\text{and } p_{Xz}^F = 2\mu UD\{1-\cos(\xi E)\}, \end{aligned}\right\} \tag{32}$$

In order to confirm the validity of the present method, the foundation input motions of an embedded square foundation in the cases of $E=B/2$ and $E=B$ are shown in Fig. 13 by comparing with the exact 3-D solutions. Both results by the proposed method exhibit a good agreement with those by the 3-D analysis especially for the horizontal motion. However a slight difference is observed in the frequency range over $a_0=\pi/2$, which corresponds to $f=V_S/4E$, in the case of $E=B$. This is due to the assumption adopted when evaluating Eq. (32) which causes the error in the high frequency range. From this reason, it is recommended that the application of the present method is limited to the system whose natural frequency is smaller than the value $V_S/4E$.

The problems including the layered soil or the neighboring foundation can also be formulated by the same approach. However, it has been pointed out that the influence of an underlying bedrock and an adjacent foundation tends to be underestimated in the approx. 3-D analysis with dashpots compared with the realistic 3-D analysis. In this paper, the application of the present method, therefore, is limited to a foundation embedded in the half-space.

CONCLUSIONS

For the purpose of evaluating effects of viscous dashpots on the soil-structure interaction, the approximate 3-D boundary element analysis was conducted and the comparison among the results of 2-D, approx. 3-D and exact 3-D analyses was made. Based on the efficiency of these dashpots, a simplified method was proposed by applying the dashpots to 1-D soil columns and the efficiency of the proposed method was examined. From these studies, the following conclusions are derived.

(1) The Green's function for the approx. 3-D problem is derived by introducing the viscous damping coefficient into the 2-D equation of motion and effects of the dashpots are examined by using the boundary element analysis.

(2) By adding dashpots, the equivalent damping of the approx. 3-D solution is re-

duced and approaches to that of 3-D one. Consequently, the approx. 3-D solutions can produce 3-D effects especially for a foundation embedded in a half-space.

(3) The influence of an underlying bedrock and an adjacent foundation tends to be underestimated by adding dashpots. By examining energy transmission, it is found that this fact is due to the excessive wave absorption.

(4) Based on the efficiency of the dashpots for a foundation embedded in a half-space, a simplified technique to evaluate the foundation input motions as well as the impedance functions is proposed by applying the dashpots to the soil columns which correspond to the soil around the foundation.

(5) The proposed method gives a good approximation to the 3-D solutions in the case that the natural frequency of a system is smaller than the values $V_S/4B$ and $V_S/4E$ and in the case that the rotational response is not so dominant. Since the proposed analysis is easily carried out even by hand calculation, this method may give us good insight for complicated problems.

ACKNOWLEDGEMENTS

We express our gratitude to Mr. Kazuhiro Yoshida and Mr. Hiroshi Kawase for offering their numerical results by the three-dimensional boundary element analysis. We also thank to Dr. Fumio Yamazaki for reviewing the draft of this paper.

REFERENCES

1) Brebbia, C. A. and Walker, S. (1980) : Boundary Element Techniques in Engineering, Newnes-Butterworths.
2) Ewing, W. M., Jardetzky, W. S. and Press, F. (1957) : Elastic Waves in Layered Media, McGraw-Hill.
3) Fukuwa, N., Hasegawa, M., Takada, T., Satoh, T., Naraoka, K. and Koyanagi, Y. (1984) : "Analysis system for soil-structure interaction by finite element method," Proc. 6 th Symp. Use Comp. Build. Eng. in Japan, pp. 85-90 (in Japanese).
4) Fukuwa, N. and Nakai, S. (1988) : "A simplified analysis method for soil structure interaction," Technical Research Report of Shimizu Corporation, Vol. 47, pp. 47-58 (in Japanese).
5) Gazetas, G. (1983) : "Analysis of machine foundations : state of the art," Int. J. Soil Dyn. Earthquake Eng., Vol. 2, pp. 1-42.
6) Gazetas, G. and Dobry, R. (1984) : "Simple radiation damping model for piles and footings," J. Eng. Mech. Div. ASCE, Vol. 110, pp. 937-956.
7) Hwang, R. N., Lysmer, J. and Berger, E. (1975) : "A simplified three dimensional soil-structure interaction study," Proc. 2 nd ASCE Specialty Conference on Structural Design of Nuclear Plant Facilities, I-A, New Orleans.
8) Jakub, M. and Roesset, J. M. (1977) : "Dynamic stiffness of foundations : 2 D vs 3 D solutions," Research Report R 77-36, MIT.
9) Kausel, E. (1974) : "Forced vibrations of circular foundations on layered media," Research Report R 74-11, MIT.
10) Lamb, H. (1904) : "On the propagation of tremors over the surface of an elastic solid," Philosophical Transaction of the Royal Society of London, A 203, pp. 1-42.
11) Love, A. E. H. (1927) : A Treatise on the Mathematical Theory of Elasticity, Dover Publication.
12) Luco, J. E. and Hadjian, A. H. (1974) : "Two-dimensional approximation of the three-dimensional soil-structure interaction problem," Nucl. Eng. Des. Vol. 31, pp. 195-203.
13) Luco, J. E. and Westmann, R. A. (1972) : "Dynamic response of a rigid footing bonded to an elastic half space," J. Appl. Mech., Vol. 39, pp. 527-534.
14) Lysmer, J. (1965) : "Vertical motions of rigid footings," Ph. D. Thesis, University of Michigan.
15) Lysmer, J., Udaka, T., Tsai, C-F. and Seed, H. B. (1975) : "FLUSH-A computer program for approximate 3-D analysis of soil-structure interaction problems," Report No. EERC 75-30, University of California, Berkeley.
16) Matsuoka, O. and Yahata, K. (1980) : "Basic analyses on problems of a three dimensional homogeneous, isotropic, elastic medium, and the applications," Trans. of Architectural Institute of Japan, No. 298, pp. 43-53 (in Japanese).
17) Meek, J. W. and Veletsos, A. S. (1974) : "Simple models in foundations of lateral and rocking motion," Proc. 5 th World Conf. Earthquake

Eng., Rome, Vol. 2, pp. 2610-2613.

18) Nakai, S. and Fukuwa, N. (1984) : "Boundary element analysis of approximate three-dimensional soil-structure interaction : Dynamic behavior of a surface foundation," Trans. of Architectural Institute of Japan, No. 344, pp. 81-92 (in Japanese).

19) Nakai, S. and Fukuwa, N. (1987) : "Boundary element analysis of approximate three-dimensional soil-structure interaction (Part II) : Approximate three-dimensional effect on soil-embedded structures interaction," Trans. of Architectural Institute of Japan, No. 380, pp. 57-67 (in Japanese).

20) Pao, Y-H. and Mow, C-C. (1971) : Diffraction of Elastic Waves and Dynamic Stress Concentrations, Crane Russak, N. Y.

21) Pauw, A. (1953) : "A dynamic analogy for foundation-soil systems," Symp. Dyn. Test. Soils, pp. 90-112.

22) Richart, F. E., Woods, R. D. and Hall, J. R. (1970) : Vibrations of Soils and Foundations, Prentice-Hall, Englewood Cliffs, N. J.

23) Wolf, J. P. and Somaini, D. R. (1986) : "Approximate dynamic model of embedded foundation in time domain," Earthquake Eng. Struct. Dyn., Vol. 14, pp. 683-703.

24) Yoshida, K. and Kawase, H. (1986) : "Dynamic cross-interaction of embedded foundations," Proc. 7 th Japanese Earthquake Engrg. Symp., pp. 1045-1050 (in Japanese).